



## Studies of Ferroelectric and Magnetic Phase Transitions in Multiferroic $\text{PbFe}_{0.5}\text{Ta}_{0.5}\text{O}_3$

I. P. Raevski, M. S. Molokeeov, S. V. Misyul, E. V. Eremin, A. V. Blazhevich, S. P. Kubrin, D. A. Sarychev, V. V. Titov, H. Chen, C.-C. Chou, S. I. Raevskaya & M. A. Malitskaya

To cite this article: I. P. Raevski, M. S. Molokeeov, S. V. Misyul, E. V. Eremin, A. V. Blazhevich, S. P. Kubrin, D. A. Sarychev, V. V. Titov, H. Chen, C.-C. Chou, S. I. Raevskaya & M. A. Malitskaya (2015) Studies of Ferroelectric and Magnetic Phase Transitions in Multiferroic  $\text{PbFe}_{0.5}\text{Ta}_{0.5}\text{O}_3$ , *Ferroelectrics*, 475:1, 52-60, DOI: [10.1080/00150193.2015.995009](https://doi.org/10.1080/00150193.2015.995009)

To link to this article: <https://doi.org/10.1080/00150193.2015.995009>



Published online: 11 Mar 2015.



Submit your article to this journal [↗](#)



Article views: 112



View related articles [↗](#)



View Crossmark data [↗](#)



Citing articles: 18 View citing articles [↗](#)

# Studies of Ferroelectric and Magnetic Phase Transitions in Multiferroic $\text{PbFe}_{0.5}\text{Ta}_{0.5}\text{O}_3$

I. P. RAEVSKI,<sup>1,\*</sup> M. S. MOLOKEEV,<sup>2</sup> S. V. MISYUL,<sup>3</sup>  
E. V. EREMIN,<sup>2</sup> A. V. BLAZHEVICH,<sup>1</sup> S. P. KUBRIN,<sup>1</sup>  
D. A. SARYCHEV,<sup>1</sup> V. V. TITOV,<sup>1</sup> H. CHEN,<sup>4</sup> C.-C. CHOU,<sup>5</sup>  
S. I. RAEVSKAYA,<sup>1</sup> AND M. A. MALITSKAYA<sup>1</sup>

<sup>1</sup>Faculty of Physics and Research Institute of Physics, Southern Federal University, 344090 Rostov-on-Don, Russia

<sup>2</sup>Kirensky Institute of Physics, Siberian Branch of the Russian Academy of Sciences, 660036 Krasnoyarsk, Russia

<sup>3</sup>Siberian Federal University, 660041 Krasnoyarsk, Russia

<sup>4</sup>Faculty of Science and Technology, University of Macau, Macau, China

<sup>5</sup>National Taiwan University of Science and Technology, Taipei, Taiwan

*X-ray, magnetic, and Mossbauer studies of a  $\text{PbFe}_{0.5}\text{Ta}_{0.5}\text{O}_3$  powder have been carried out. For the first time temperature dependence of the unit cell parameters was obtained. Antiferromagnetic Neel temperature  $T_N \approx 180$  K was determined using the results of Mossbauer studies. In the vicinity of  $T_N$  an anomaly in the temperature dependence of the monoclinic angle  $\beta$  was revealed in PFT. This anomaly seems to be due to the magnetoelectric coupling.*

**Keywords** Lead iron tantalate; multiferroic; ferroelectric; lattice parameters; phase transition

## 1. Introduction

Lead iron tantalate  $\text{PbFe}_{0.5}\text{Ta}_{0.5}\text{O}_3$  (PFT) is a multiferroic possessing simultaneously ferroelectric and magnetic properties [1–3]. At present, multiferroics are in the very focus of materials science due to possibility of converting the magnetic signals to electric responses and vice versa. PFT-based solid solutions are among the best candidates for such applications as they were reported to possess a large magnetoelectric response and low dielectric losses at room temperature [2]. PFT was one of the first multiferroics discovered by Smolenskii et.al. [3]. In majority of studies the symmetry of PFT at room temperature was reported to be cubic. For the low-temperature phase of PFT the rhombohedral ( $R\bar{3}m$ ) symmetry was reported at first in Refs. [4, 5]. However, at present it is generally adopted that on cooling PFT undergoes phase transitions from the cubic paraelectric ( $Pm\bar{3}m$ ) to tetragonal ferroelectric ( $P4mm$ ) phase at  $T_{C1} = 240\text{--}270$  K, and then to the monoclinic ferroelectric ( $Cm$ ) phase, at  $T_{C2} = 200\text{--}220$  K [6–8]. It should be noted

---

Received July 15, 2014; Accepted September 30, 2014.

\*Corresponding author. E-mail: igorraevsky@gmail.com

Color versions of one or more of the figures in the article can be found online at [www.tandfonline.com/lfnn](http://www.tandfonline.com/lfnn).

that up to now the temperature dependence of the unit cell parameters for PFT has not been determined. In Ref. [6] the dependence of interplanar distances on temperature has been measured for PFT single crystal in order to determine the phase transition temperatures, while in other works the structure refinement has been carried out only for a few temperatures [4, 5, 7]. Besides two structural phase transitions, PFT undergoes also a transition into the G-type antiferromagnetic phase. The temperature of this transition (the Neel temperature,  $T_N$ ) determined in different works varies from 130 to 180 K [4, 9, 10], while at much lower temperature (10–20 K) a transition into a spin glass state was reported [8, 11]. The temperature of magnetic phase transition in Fe-containing oxides is believed to depend on the number of possible Fe–O–Fe linkages in the crystal lattice [12]. In ternary  $PbFe_{0.5}M^{5+}_{0.5}O_3$  perovskites this number can be governed, e.g. by changing the degree S of  $Fe^{3+}$  and  $M^{5+}$  ordering, as the ordering changes the number of magnetic ions in the neighboring unit cells and thus reduces the possible number of Fe–O–Fe linkages. However, in contrast to  $PbM^{3+}_{0.5}M^{5+}_{0.5}O_3$  perovskites with  $M^{3+}$ - Sc, Yb;  $M^{5+}$ - Nb, Ta [13, 14], no superstructure reflections on X-ray diffraction patterns due to M-cation ordering have been reported for PFT [4–7]. At the same time, the experimental value of  $T_N$  for PFT is located approximately halfway between calculated values of this temperature for the fully ordered ( $T_N = 0$  K) and completely disordered ( $T_N \approx 300$  K) states [4]. This fact is usually interpreted as an evidence of a partial ordering of  $Fe^{3+}$  and  $Ta^{5+}$  cations [4]. The possible reason for the absence of superstructural reflections on X-ray diffraction patterns is a local character of ordering in PFT i.e., mesoscopic domains of several nanometers in size with different values of S coexist in a crystal. Magnetic phase transition temperature in PFT and in its analog  $PbFe_{0.5}Nb_{0.5}O_3$  (PFN) is more than 100 K higher as compared to similar lead-free  $AFe_{0.5}M^{5+}_{0.5}O_3$  (A-Ca, Sr, Ba;  $M^{3+}$ -Nb, Ta) perovskites [15]. This dramatic difference is attributed to the possibility of magnetic superexchange via an empty 6p state of  $Pb^{2+}$  ions [15] or to the clustering of Fe ions. According to first-principle calculations [16], clustering of Fe ions appears to be more probable in  $PbFe_{0.5}M^{5+}_{0.5}O_3$  ( $M^{5+}$ -Nb, Ta) compounds than in their lead-free counterparts. So, the possible reason of the large scattering of  $T_N$  values obtained for PFT in different works seems to be a local compositional ordering and/or clustering of Fe ions. Studies of  $^{93}Nb$  and  $^{17}O$  NMR [17] and  $^{57}Fe$  Mossbauer spectra [16] as well as first-principal calculations [16] have led to the conclusion that PFN is a chemically inhomogeneous system and a long range antiferromagnetic order develops in Fe-rich-Nb-poor regions while, a magnetic relaxor spin-glass like state below  $T \approx 10$ –20 K can arise from the Fe-poor-Nb-rich regions. Similar scenario seems to be valid for PFT.

For several multiferroics, e.g., PFN [18],  $PbFe_{2/3}W_{1/3}O_3$  [19],  $RMn_2O_5$  (R-Tb, Ho, and Dy) [20, 21], anomalies in the temperature dependences of lattice parameters in the vicinity of  $T_N$  have been reported. These anomalies are supposed to be due to the magnetoelectric coupling [1, 18]. However, no attempt has been made so far to look for similar anomalies in the unit cell parameters in PFT.

The scope of the present paper is to study the temperature changes of the unit cell parameters, magnetization, and Mossbauer spectra for PFT powder with special emphasis on the temperature range of the antiferromagnetic phase transition.

## 2. Experimental

All the known low-temperature X-ray or neutron diffraction studies of PFT have been carried out using the flux-grown single crystals or a powder obtained by crushing such crystals [4–7]. This is due to the difficulties connected with obtaining the

single-phase perovskite PFT by the solid-state reaction route. In particular, in contrast to  $\text{PbMg}_{1/3}\text{Nb}_{2/3}\text{O}_3$ , PFN, and some other ternary perovskites, in the case of PFT even the use of presintered wolframite  $\text{FeTaO}_4$  precursor for solid state synthesis does not provide significant benefits as compared to the synthesis from the mixture of oxides [2, 3, 8, 9]. However, in Ref. [22] single phase perovskite PFT was obtained by solid state synthesis from the mixture of  $\text{Fe}_2\text{O}_3$  and  $\text{Ta}_2\text{O}_5$  using  $\text{PbCO}_3$  instead of  $\text{PbO}$  and adding 10 wt.% excess of  $\text{PbCO}_3$  for lead loss compensation. We used just this method for the synthesis of PFT. High-purity  $\text{Fe}_2\text{O}_3$ ,  $\text{PbCO}_3$ , and  $\text{Ta}_2\text{O}_5$  were batched in stoichiometric proportions and mixed thoroughly together with 10 wt.% excess of  $\text{PbCO}_3$  in an agate mortar in the presence of ethyl alcohol. Then the synthesis was carried out for 4 h at 850 °C. After the synthesis the product of reaction was crushed by pestle in an agate mortar. The PFT powder was annealed for 2 hours at 450 °C to eliminate possible residual mechanical stresses.

For comparison, in some experiments Li-doped PFT ceramics was studied. It was sintered at 1100 °C from the mixture of  $\text{PbO}$  and  $\text{FeTaO}_4$  with addition of 5 mol.% of  $\text{Li}_2\text{CO}_3$  [10]. Li-doping is known to stimulate the formation of the perovskite phase and reduce the conductivity in both PFN and PFT ceramics [10].

Mossbauer spectra were measured on powders (5-10 mg/cm<sup>2</sup>) at natural <sup>57</sup>Fe isotope content with the aid of an MS-1104E rapid spectrometer of the latest design and analyzed using the original computer program UNIVEM [10]. The isomer chemical shifts were determined with respect to metallic  $\alpha$ -Fe. Magnetic measurements were performed using the PPMS-9 physical property measurement system (Quantum Design) in the temperature range 2–350K and under magnetic field up to 90 kOe.

The X-ray diffraction study of the PFT powder was performed on a D8-ADVANCE diffractometer ( $\text{CuK}_\alpha$  radiation,  $\theta$ - $2\theta$  scan mode) using a VANTEC linear detector and a TTK 450 Anton Paar temperature chamber in the 130-300 K temperature range. The scan step in the angle  $2\theta$  was 0.016°.

### 3. Results and Discussion

X-ray diffraction studies have shown that the synthesized PFT powder was single-phase and had a structure of the perovskite type. X-ray pattern at room temperature is shown in Fig. 1. Two very small extra reflections in the 30–40 deg. range seem to correspond to the traces of orthorhombic  $\text{PbO}$  (the American Society for Testing Materials (ASTM) code 72-93), as the starting mixture contained some excess of  $\text{PbCO}_3$  to compensate the  $\text{PbO}$  evaporation during the synthesis.

In our experiments, similar to the data reported in Refs. [6, 7], cooling the sample below  $T_{C1}$  ( $\approx 270$  K) and then below  $T_{C2}$  ( $\approx 220$  K) resulted in a slight broadening of the X-ray diffraction peaks indicating a change in the point symmetry. However, the superstructure reflections, which would indicate a change of translational symmetry, were not observed in the X-ray diffraction patterns below 270 K. Thus, our structural data, as well as the data reported in Refs. [6, 7], indicate a change of the point symmetry and the lack of the translational symmetry changes, i.e. unit cell volume of the cubic phase, at the phase transitions.

For PFT powder the unit cell parameters in all the temperature points within the 135-360 K range were obtained by fitting the X-ray diffraction profiles using the set of codes TOPAS 4.2 [23]. The obtained temperature dependence of the PFT unit cell parameters is shown in Fig. 2. One can see the anomalies of the unit cell parameters at  $T_{CT} \approx 270$  K and  $T_{TM} \approx 220$  K. Similar anomalies can be seen on the temperature dependence of the unit cell volume (Fig. 3). It should be mentioned that the monoclinic angle  $\beta$  shows the

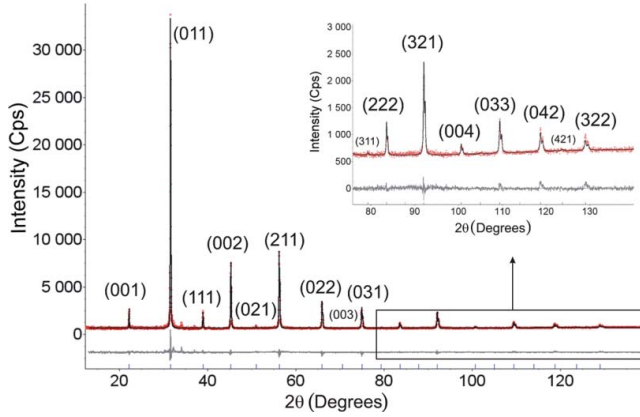


**Figure 1.** X-ray pattern of PFT powder at 300K. Red line represents experimental pattern, black line shows the simulated X-ray picture, gray line at the bottom shows the difference between experimental and simulated data.

unusual temperature dependence. On cooling its value at first remains nearly constant or even lowers, but below approximately 180 K it begins to increase and becomes close to  $90^\circ$  (Fig. 4). This unusual behavior will be discussed in more details further.

Figure 5 shows the temperature dependences of magnetization  $M$  for the PFT powder and Li-doped PFT ceramics. For Li-doped ceramics the  $M(T)$  dependence is very similar to the one reported for PFT and PFN single crystals [4, 9, 11, 24] and PFT ceramics [25]: on heating under a magnetic field of 1 kOe after zero field cooling (ZFC) magnetization exhibits a maximum at 16 K. Besides this maximum, there is also a bump on the  $M(T)$  curve at about 130 K. It is well documented that such a bump in PFN and PFT corresponds to  $T_N$  [4, 9, 11, 24, 25]. Thus, obtained  $T_N \approx 130$  K falls within the range of  $T_N$

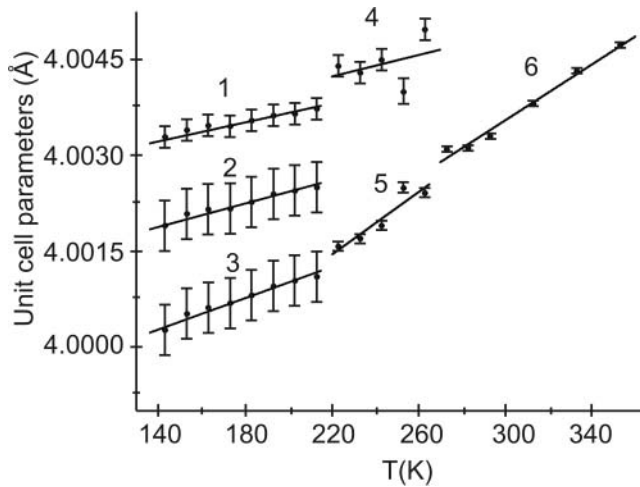


**Figure 2.** Temperature dependences of the unit cell parameters for PFT powder in the monoclinic  $Cm$ , tetragonal  $P4mm$ , and cubic  $Pm\bar{3}m$  phases: 1 -  $c_{mon}$ ; 2 -  $a_{mon}/\sqrt{2}$ ; 3 -  $b_{mon}/\sqrt{2}$ ; 4 -  $c_{tetr}$ ; 5 -  $a_{tetr}$ ; 6 -  $a_{cub}$ .

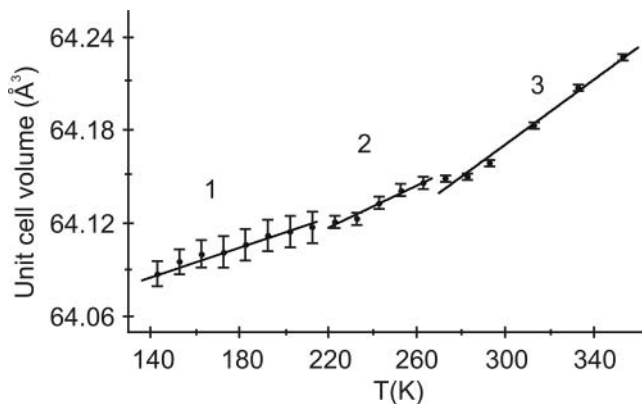


**Figure 3.** Temperature dependence of the unit cell volume for PFT powder. 1 –  $V_{\text{mon}}/2$ ; 2 –  $V_{\text{tet}}$ ; 3 –  $V_{\text{cub}}$ .

values reported for PFT in the literature [4, 9, 10]. Previously, we revealed that the  $T_N$  values of Li-doped PFT ceramics depend on the sintering temperature and are often lower than those of single crystals and undoped ceramics due to possible partial ordering of Fe and Ta ions [10] or/and to a change in the degree of Fe-ions clustering [16]. The  $M(T)$  dependence measured for Li-doped PFT ceramics in the field-cooled (FC) mode nicely coincides with the one measured in the ZFC mode except a low-temperature region where the FC curve does not show a maximum. Such a difference between the  $M(T)$  curves measured in the ZFC and FC modes is typical for a spin-glass state [11, 24].

Li-doped PFT ceramics exhibits slim magnetic hysteresis loops at very low temperatures of about few K (Fig. 6a). However, at 50 K, that is well below the Neel temperature, the  $M(H)$  dependence shows only a slight nonlinearity, while at higher temperatures, namely at 100 and 150 K it is practically linear. Thus, the evolution of magnetic

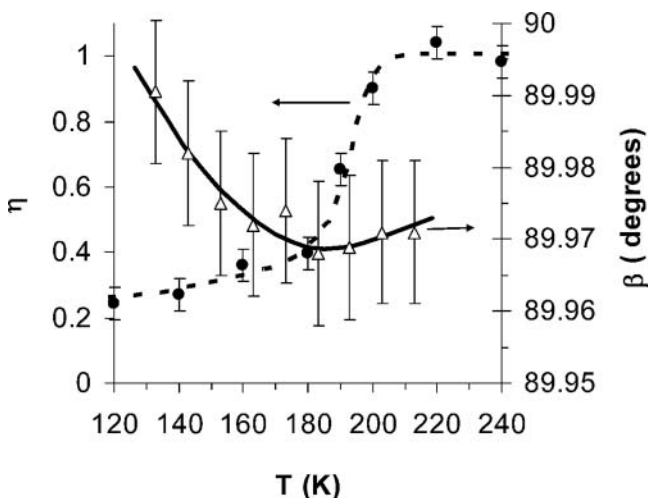


**Figure 4.** Temperature dependences of the monoclinic angle  $\beta$  and  $\eta$ -Mossbauer spectra intensity within the 0-1.2 mm/s velocity range normalized to its value at 300 K, for PFT powder.

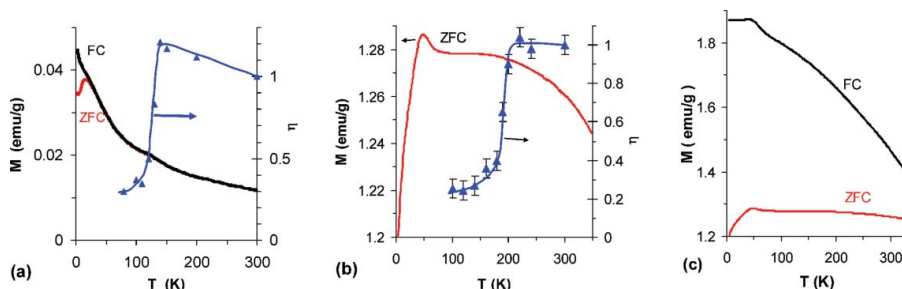


**Figure 5.** Temperature dependences of magnetization  $M$  measured under a magnetic field of 1kOe in the ZFC and FC modes and  $\eta$ -Mossbauer spectra intensity within the 0-1.2 mm/s velocity range normalized to its value at 300 K, for Li-doped PFT ceramics (a) and PFT powder (b, c).

hysteresis loops with temperature for Li-doped PFT ceramics is very similar to the data obtained for PFN single crystal [24].

PFT powder exhibited unusually high magnetization values which were more than an order of magnitude larger as compared to Li-doped PFT ceramics (Fig. 5b), PFT ceramics studied in Ref. [25], and single crystals of PFT [11] and PFN [24]. No distinct anomalies are seen in the ZFC magnetization-temperature curve of PFT powder in the 50-350 K temperature range. In contrast to Li-doped PFT ceramics, PFT [11], and PFN [24] single crystals, the ZFC and FC magnetization-temperature curves for PFT powder did not coincide at high temperatures (Fig. 5c) and were much more diffused. For the ZFC curve of Li-doped PFT ceramics the ratio of the  $M(T)$  maximal value to the  $M$  value at 300 K is about 3.3, while the same ratio for the PFT powder does not exceed 1.02. The PFT powder exhibited well-defined magnetic hysteresis  $M(H)$  loops (Fig. 6b) up to at least 150 K (the maximal temperature at which the loops were measured). As these loops change rather weakly from 3 K to 150 K (Fig. 6b) and significant difference between ZFC and FC curves persists at least up to 350 K (Fig. 5c), it seems that the loops would exist at room temperature as well. It is worth noting that very high magnetization values and similar shape of magnetization-temperature curve as well as the presence of magnetic hysteresis loops up to room temperature have been reported recently [8] for PFT ceramic sample. We suppose that such unusual

**Figure 6.** Magnetic hysteresis loops measured at 3 K, 50 K, 100 K, and 150 K (from the uppermost to lowermost one) for Li-doped PFT ceramics (a) and PFT powder (b). The inset in panel (b) shows the low-field portion of the hysteresis loop for PFT powder at 150 K.

behavior is due to the presence in the PFT powder studied in the present work as well as in PFT ceramics studied in Ref. [8] of a small amount of ferrimagnetic impurity, presumably lead hexaferrite  $\text{PbFe}_{12}\text{O}_{19}$ . Though the content of this impurity seems to be well below the detection limit of the X-ray diffraction analysis, ferrimagnetic impurity has a great impact on the magnetic properties of the antiferromagnetic or paramagnetic matrix. This assumption is supported by the fact that very similar diffused  $M(T)$  curves were observed for the magnetoelectric composite based on ferrimagnetic  $\text{Ni}_{0.3}\text{Zn}_{0.62}\text{Cu}_{0.08}\text{Fe}_2\text{O}_4$  ferrite as a magnetostrictive phase and  $\text{Pb}(\text{Fe}_{0.5}\text{Nb}_{0.5})\text{O}_3$  as a piezoelectric phase [26].

Thus, we failed to determine the Neel temperature of the PFT powder under study from the magnetization data. So, we used Mossbauer spectroscopy for this purpose.

At room temperature Mossbauer  $^{57}\text{Fe}$  spectra of both the PFT powder and Li-doped PFT ceramics studied appeared to be doublets with quadrupole splitting of 0.44 mm/s and isomer shift of 0.4 mm/s (relative to metallic iron), corresponding to the  $\text{Fe}^{3+}$  ions occupying the octahedral sites of perovskite lattice. When cooled below the Neel temperature,  $T_N$ , the Mossbauer spectrum transforms from doublet to sextet [10]. This transformation is accompanied by a dramatic decrease of the magnitude  $\eta$  of Mossbauer spectra intensity within the 0–1.2 mm/s velocity range normalized to its value at 300 K (Figs. 4, 5). Using the 0–1.2 mm/s velocity range instead of a fixed velocity value as a reference point enables us to take into account a possible change of isomer shift and/or quadrupole splitting with temperature. It should be also noted that finite  $\eta$  values observed at  $T < T_N$  (panels a and b in Fig. 5) are due not only to the presence of a part of iron ions in the magnetically disordered state, but rather to the contribution of the sextet component of the spectrum falling within the 0–1.2 mm/s velocity range. The abrupt drop in the temperature dependence of  $\eta$  allows one to obtain  $T_N$  from the Mossbauer experiment. This method was successfully used previously to determine  $T_N$  values for several multiferroics and the results obtained appeared to be very similar to the data obtained by traditional methods, such as measuring the temperature dependence of magnetization or the line width of the electron spin resonance spectrum [10, 17, 24]. Indeed, as one can see from Fig. 5a, for Li-doped PFT ceramics the temperature of the  $\eta(T)$  anomaly nicely coincides with the bump in the magnetization-temperature curve. For PFT powder the Mossbauer data give the Neel temperature value about 180–190 K (Fig. 4), which agrees with some data published for PFT [4]. It is worth noting that this  $T_N$  value coincides well with the temperature, at which the minimum in the temperature dependence of the monoclinic angle  $\beta$  is observed for the same PFT powder (Fig. 4). Around 180 K one can also see some small anomalies in the temperature dependence of the monoclinic unit cell parameters (Fig. 2); however, these anomalies are within the experimental error. For a more reliable data one needs to use a synchrotron X-ray diffraction study. It seems that the observed minimum in the  $\beta(T)$  dependence and tiny anomalies of the unit cell parameters are similar to the anomalies observed at  $T_N$  in other multiferroics [18–21]. These anomalies are usually ascribed to the magnetoelectric coupling, which is believed to maximize in the vicinity of  $T_N$  [1]. This coupling may be either direct (between electrical and magnetic order parameters) or indirect (via lattice strain) [18, 27]. In principle, the last mechanism may enhance the magnetoelectric coupling substantially, as observed in some composites [26, 27].

#### 4. Summary

In summary, single phase perovskite powder of lead iron tantalate  $\text{PbFe}_{0.5}\text{Ta}_{0.5}\text{O}_3$  (PFT) was synthesized via a solid state reaction route using  $\text{PbCO}_3$ ,  $\text{Fe}_2\text{O}_3$ , and  $\text{Ta}_2\text{O}_5$  as starting



compounds. For the first time the temperature dependence of the unit cell parameters was obtained for PFT using X-ray powder diffraction. Antiferromagnetic Neel temperature  $T_N \approx 180$  K was determined using the results of Mossbauer studies. In the vicinity of  $T_N$  an anomaly in the temperature dependence of the monoclinic angle  $\beta$  was revealed in PFT. Similar to other known multiferroics, this anomaly is presumably due to the magnetoelectric spin-lattice coupling.

## Funding

This study is partially supported by the Russian Foundation for Basic Research (RFBR) project (projects 12-08-00887\_a and 14-02-90438\_Ucr\_a), Ministry of education and science of Russian Federation (research project 2132, task 2014/174), Southern Federal University grant 213.01-2014/012-VG and Research Committee of the University of Macau under Research & Development Grant for Chair Professor.

## References

1. G. A. Smolenskii and I. E. Chupis, *Ferroelectromagnets*. *Sov. Phys. Usp.* **25**, 475–493 (1982).
2. D. A. Sanchez, N. Ortega, A. Kumar, R. Roque-Malherbe, R. Polanco, J. F. Scott, and R. S. Katiyar, Symmetries and multiferroic properties of novel room-temperature magnetoelectrics: Lead iron tantalate – lead zirconate titanate (PFT/PZT). *AIP Advances*. **1**, 042169 (2011).
3. G. A. Smolenskii, A. I. Agranovskaia, and V. A. Isupov, New ferroelectrics of complex composition  $Pb_2MgWO_6$ ,  $Pb_3Fe_2WO_9$ ,  $Pb_2FeTaO_6$ . *Sov. Phys. Solid State*. **1**, 907–909 (1959).
4. S. Nomura, H. Takabayashi, and T. Nakagawa, Dielectric and magnetic properties of  $Pb(Fe_{1/2}Ta_{1/2})O_3$ . *Jap. J. Appl. Phys.* **7**, 600–604 (1968).
5. S. A. Ivanov, S. Eriksson, N. W. Thomas, R. Tellgren, and H. Rundlof, A neutron powder diffraction study of the ferroelectric relaxor  $Pb(Fe_{1/2}Ta_{1/2})O_3$ . *J. Phys.: Condens. Matter*. **13**, 25–33 (2001).
6. A. Geddo-Lehmann and P. Sciau, Ferroelastic symmetry changes in the perovskite  $PbFe_{0.5}Ta_{0.5}O_3$ . *J. Phys.: Condens. Matter*. **11**, 1235–1245 (1999).
7. N. Lampis, P. Sciau, and A. Geddo-Lehmann, Rietveld refinements of the paraelectric and ferroelectric structures of  $PbFe_{0.5}Ta_{0.5}O_3$ . *J. Phys.: Condens. Matter*. **12**, 2367–2378 (2000).
8. R. Martinez, R. Palai, H. Huhtinen, J. Liu, J. F. Scott, and R. S. Katiyar, Nanoscale ordering and multiferroic behavior in  $PbFe_{1/2}Ta_{1/2}O_3$ . *Phys. Rev. B*. **82**, 134104 (2010).
9. L. I. Shvorneva and Yu. N. Venevtsev, Perovskites with ferroelectromagnetic properties. *Sov. Phys. JETP*. **22**, 722–726 (1965).
10. I. P. Raevski, S. P. Kubrin, S. I. Raevskaya, V. V. Stashenko, D. A. Sarychev, M. A. Malitskaya, M. A. Sereckina, V. G. Smotrakov, I. N. Zakharchenko, and V. V. Eremkin: Dielectric and Mossbauer studies of perovskite multiferroics. *Ferroelectrics*. **373**, 121–126 (2008).
11. A. Falqui, N. Lampis, A. Geddo-Lehmann, and G. Pinna, Low-temperature magnetic behavior of perovskite compounds  $PbFe_{1/2}Ta_{1/2}O_3$  and  $PbFe_{1/2}Nb_{1/2}O_3$ . *J. Phys. Chem.* **B109**, 22967–22970 (2005).
12. M. A. Gilleo, Superexchange interaction in ferromagnetic garnets and spinels which contain randomly incomplete linkages. *J. Phys. Chem. Sol.* **13**, 33–39 (1960).
13. A. A. Bokov, V. Yu. Shonov, I. P. Raevsky, E. S. Gagarina, and M. F. Kupriyanov, Compositional ordering and phase transitions in  $PbYb_{1/2}Nb_{1/2}O_3$ . *J. Phys. Condens. Matter*. **5**, 5491–5504 (1993).
14. I. P. Raevski, S. A. Prosandeev, S. M. Emelyanov, V. G. Smotrakov, V. V. Eremkin, I. N. Zakharchenko, S. I. Raevskaya, E. S. Gagarina, F. I. Savenko, and E. V. Sahkar, Comparative study of cation ordering effects in single crystals of 1:1 and 1:2 complex perovskites solid solutions. *Ferroelectrics*. **298**, 267–274 (2004).

15. I. P. Raevski, S. P. Kubrin, S. I. Raevskaya, V. V. Titov, D. A. Sarychev, M. A. Malitskaya, I. N. Zakharchenko, and S. A. Prosandeev, Experimental evidence of the crucial role of nonmagnetic Pb cations in the enhancement of the Néel temperature in perovskite  $\text{Pb}_{1-x}\text{Ba}_x\text{Fe}_{1/2}\text{Nb}_{1/2}\text{O}_3$ . *Phys. Rev. B*, **80**, 024108 (2009).
16. I. P. Raevski, S. P. Kubrin, S. I. Raevskaya, D. A. Sarychev, S. A. Prosandeev, and M. A. Malitskaya, Magnetic properties of  $\text{PbFe}_{1/2}\text{Nb}_{1/2}\text{O}_3$ : Mossbauer spectroscopy and first principles calculations. *Phys. Rev. B*, **85**, 224412 (2012).
17. V. V. Laguta, J. Rosa, L. Jastrabik, R. Blinc, P. Cevc, B. Zalar, M. Remskar, S. I. Raevskaya, and I. P. Raevski,  $^{93}\text{Nb}$  NMR and  $\text{Fe}^{3+}$  EPR study of local magnetic properties of disordered magnetoelectric  $\text{PbFe}_{1/2}\text{Nb}_{1/2}\text{O}_3$ . *Mater. Res. Bull.* **45**, 1720–1727 (2010).
18. S. P. Singh, D. Pandey, S. Yoon, S. Baik, and N. Shin, Evidence for monoclinic crystal structure and negative thermal expansion below magnetic transition temperature in  $\text{Pb}(\text{Fe}_{1/2}\text{Nb}_{1/2})\text{O}_3$ . *Appl. Phys. Lett.* **90**, 242915 (2007).
19. S. A. Ivanov, S.-G. Eriksson, R. Tellgren, and H. Rundlof, Neutron powder diffraction study of the magnetoelectric relaxor  $\text{Pb}(\text{Fe}_{2/3}\text{W}_{1/3})\text{O}_3$ . *Mat. Res. Bull.* **39**, 2317–2328 (2004).
20. L. C. Chapon, G. R. Blake, M. J. Gutmann, S. Park, N. Hur, P. G. Radaelli, and S. W. Cheong, *Phys. Rev. Lett.* **93**, 107207 (2004).
21. G. R. Blake, L. C. Chapon, P. G. Radaelli, S. Park, N. Hur, S.-W. Cheong, and J. Rodríguez-Carvajal, *Phys. Rev. B*, **71**, 214402 (2005).
22. W. Z. Zhu, A. Kholkin, P. Q. Mantas, and J. L. Baptista, Preparation and characterization of  $\text{Pb}(\text{Fe}_{1/2}\text{Ta}_{1/2})\text{O}_3$  relaxor ferroelectric. *J. Eur. Ceram. Soc.* **20**, 2029–2034 (2000).
23. A. X. S. Bruker, TOPAS V4: General profile and structure analysis software for powder diffraction data. User's Manual, Bruker AXS, Karlsruhe, Germany; 2008.
24. V. V. Laguta, M. D. Glinchuk, M. Maryško, R. O. Kuzian, S. A. Prosandeev, S. I. Raevskaya, V. G. Smotrakov, V. V. Eremkin, and I. P. Raevski, Effect of the Ba and Ti-doping on the magnetic properties of multiferroic  $\text{Pb}(\text{Fe}_{1/2}\text{Nb}_{1/2})\text{O}_3$ . *Phys. Rev. B*, **87**, 064403 (2013).
25. R. N. P. Choudhury, C. Rodriguez, P. Bhattacharya, R. S. Katiyar, and C. Rinaldi, Low-frequency dielectric dispersion and magnetic properties of La, Gd modified  $\text{Pb}(\text{Fe}_{1/2}\text{Ta}_{1/2})\text{O}_3$  multiferroics. *J. Magn. Magn. Mater.* **313**, 253–260 (2007).
26. P. Guzdek, M. Sikora, L. Gora, and C. z. Kapusta, Magnetic and magnetoelectric properties of nickel ferrite–lead iron niobate relaxor composites. *J. Eur. Ceram. Soc.* **32**, 2007–2011 (2012).
27. M. H. Lente, J. D. S. Guerra, G. K. S. de Souza, B. M. Fraygola, C. F. V. Raigoza, D. Garcia, and J. A. Eiras, Nature of the magnetoelectric coupling in multiferroic  $\text{Pb}(\text{Fe}_{1/2}\text{Nb}_{1/2})\text{O}_3$  ceramics. *Phys. Rev. B*, **78**, 054109 (2008).